

LEARNING TO CROSS EXCHANGE TO SOLVE MIN-MAX VEHICLE ROUTING PROBLEMS

Minjun Kim*, Junyoung Park*, & Jinkyoo Park

KAIST, Daejeon, South Korea

{minjun1212, junyoungpark, jinkyoo.park}@kaist.ac.kr

ABSTRACT

CROSS exchange (CE), a meta-heuristic that solves various vehicle routing problems (VRPs), improves the solutions of VRPs by swapping the sub-tours of the vehicles. Inspired by CE, we propose Neuro CE (NCE), a fundamental operator of *learned* meta-heuristic, to solve various min-max VRPs while overcoming the limitations of CE, i.e., the expensive $\mathcal{O}(n^4)$ search cost. NCE employs graph neural network to predict the cost-decrements (i.e., results of CE searches) and utilizes the predicted cost-decrements to guide the selection of sub-tours for swapping, while reducing the search cost to $\mathcal{O}(n^2)$. As the learning objective of NCE is to predict the cost-decrement, the training can be simply done in a supervised fashion, whose training samples can be easily collected. Despite the simplicity of NCE, numerical results show that the NCE trained with min-max flexible multi-depot VRP (min-max FMDVRP) outperforms the meta-heuristic baselines. More importantly, it significantly outperforms the neural baselines when solving distinctive special cases of min-max FMDVRP (e.g., min-max MDVRP, min-max mTSP, min-max CVRP) without additional training.

1 INTRODUCTION

The field of neural combinatorial optimization (NCO), an emerging research area intersecting operation research and artificial intelligence, aims to train an effective solver for various combinatorial optimization (CO) problems, such as the traveling salesman problem (TSP) (Bello et al., 2016; Khalil et al., 2017; Nazari et al., 2018; Kool et al., 2018; Kwon et al., 2020), vehicle routing problems (VRPs) (Bello et al., 2016; Khalil et al., 2017; Nazari et al., 2018; Kool et al., 2018; Kwon et al., 2020; Hottung & Tierney, 2019; Lu et al., 2019; da Costa et al., 2021), and vertex covering problems (Khalil et al., 2017; Li et al., 2018; Guo et al., 2019). As NCO tackles NP-hard problems using various state-of-the-art (SOTA) deep learning techniques, it is considered an important research area in artificial intelligence. At the same time, NCO is an important field from a practical point of view because it can solve complex real-world problems. The current study mainly focuses on VRPs, a type of CO problems.

Majority of learning-based VRP solvers learns to improve the current solution to obtain a better solution (i.e., improvement heuristics) (Hottung & Tierney, 2019; Lu et al., 2019; da Costa et al., 2021) or construct a solution sequentially (i.e., construction heuristics) (Bello et al., 2016; Khalil et al., 2017; Nazari et al., 2018; Kool et al., 2018; Kwon et al., 2020; Park et al., 2021; Cao et al., 2021). To learn such solvers, learning-based methods either employ supervised learning (SL), which imitates the solutions of the verified solvers, or reinforcement learning (RL), which learn a solver from the generated routes. Most NCO studies focus on the well-established “min-sum VRP” that aims to minimize the total traveling distance of vehicles, possibly because the benchmark problems and baseline algorithms are set up for the “min-sum VRP.” On the other hand, VRP with different objectives have not received much attention from the NCO community, even though they can model various practical scenarios. For example, “min-max VRP” that aims to minimize the total completion time (i.e., makespan) of various time-critical distributed tasks (e.g., vaccine delivery, grocery delivery) has not been widely considered.

*Equal contribution

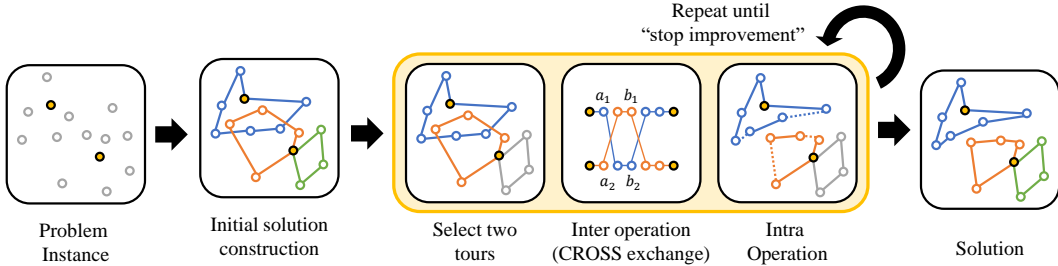


Figure 1: The overall procedure of improvement heuristic that uses CE as the inter-operation.

This study aims to learn a fundamental and universal operator that can effectively solve various practical “min-max VRP” that have flexible depot constraints. To design an universal and simple, yet powerful operator, we utilize CROSS-exchange (CE) (Taillard et al., 1997), a local search designed to conduct the inter-operation of two routes (i.e., swapping the sub-tours of two selected routes) to reduce the traveling cost. We noticed that the inter-operation of CE is especially effective in improving the quality of “min-max VRP” because it can consider the interaction among multiple vehicles, and effectively reduce the differences between the traveling distances of all vehicles. However, the search cost for selecting the sub-tours from two trajectory is $\mathcal{O}(n^4)$ where n is the tour length. This make CE unapplicable to large scale VRPs.

In this paper, we propose Neuro CE (NCE) that effectively conducts the CE operation with significantly less computational complexity. NCE amortizes the search for ending nodes of the sub-tours by employing a graph neural network (GNN), which predicts the best cost decrement, given two starting nodes from two given trajectories. NCE searches over only promising starting nodes using the prediction. Hence, the proposed NCE has $\mathcal{O}(n^2)$ search complexity. Furthermore, unlike other SL or RL approaches, the prediction target labels of NCE is not the entire solution of the VRPs, but the cost decrements of the CE operations (true target operator), which makes the collection of training data simple and easy.

The contributions of this study are summarized as follows:

- **Generalizability/Transferability:** As NCE learns a fundamental and universal operator to solve various complex min-max VRPs without retraining for each type of VRPs.
- **Trainability:** The NCE operator is trained in a supervised manner with the dataset comprised of the tour pairs and cost decrements, which make the collection of training data easy and simple.
- **Practicality/Performance:** We evaluate NCE with various types of min-max VRPs, including flexible multi-depot VRP (min-max FMDVRP), multi-depot VRP (min-max MDVRP), multiple TSP (min-max mTSP), and capacitated VRP (min-max CVRP). Extensive numerical experiments validate that NCE outperforms SOTA meta-heuristics and NCO baselines in solving various min-max VRPs, even though NCE is only trained with the data from min-max FMDVRP.

2 PRELIMINARIES

This section introduces the target problem, min-max flexible multi-depot VRP (min-max FMDVRP), and the CE operator, a powerful local-search heuristics that solves min-max FMDVRP.

2.1 MIN-MAX FLEXIBLE MULTI-DEPOT VRP

Min-max FMDVRP is a generalization of VRP that aims to find the coordinated routes of multiple vehicles with multiple depots. The flexibility allows vehicles to go back to any depots regardless of their starting depots. The min-max FMDVRP is formulated as follows:

$$\min_{\pi \in \mathbb{S}(P)} \max_{i \in \mathbb{V}} C(\tau_i) \quad (1)$$

where P is the description of the min-max FMDVRP instance that is composed of a set of vehicles \mathbb{V} , $\mathbb{S}(P)$ is the set of solutions that satisfy the constraints of the min-max FMDVRP (i.e., feasible solutions), and $\pi = \{\tau_i\}_{i \in \mathbb{V}}$ is a solution of the min-max FMDVRP. The tour $\tau_i = [N_1, N_2, \dots, N_{l(i)}]$

Algorithm 1: Neuro CROSS exchange (NCE) for solving VRP family

Input: VRP instance P , cost-decrement prediction model f_θ , Perturbation parameter p
Output: Optimized tours $\{\tau_i^*\}_{i \in |\mathbb{V}|}$

```

1  $\{\tau_i\}_{i \in |\mathbb{V}|} \leftarrow \text{GetInitialSolution}(P)$ 
2  $C_{\text{per}} \leftarrow 0$ 
3 while True do
4   while improvement do
5      $(\tau_1, \tau_2) \leftarrow \text{SelectTours}(\{\tau_i\}_{i \in |\mathbb{V}|})$ 
6      $(\tau'_1, \tau'_2) \leftarrow \text{NeuroCROSS}(\tau_1, \tau_2, f_\theta)$  // Inter operation
7      $\tau'_i \leftarrow \text{IntraOperation}(\tau_i), i = 1, 2$ 
8      $\tau_1 \leftarrow \tau'_1, \tau_2 \leftarrow \tau'_2$ 
9   if update then
10     $\{\tau_i^*\}_{i \in |\mathbb{V}|} \leftarrow \{\tau_i\}_{i \in |\mathbb{V}|}$ 
11  if  $C_{\text{per}} = p$  then
12    break
13   $C_{\text{per}} \leftarrow C_{\text{per}} + 1$ 
14   $(\tau_1, \tau_2) \leftarrow \text{ChooseRandomTours}$ 
15   $(\tau_1, \tau_2) \leftarrow \text{RandomExchange}(\tau_1, \tau_2)$  // escape from local minima
```

of vehicle i is the ordered collection of the visited tasks by the vehicle v_i , and $C(\tau_i)$ is the cost of τ_i . Min-max FMDVRP can be used to formulate the operation of shared vehicles that can be picked up from or delivered to any depots. The mixed integer linear programming (MILP) formulation of min-max FMDVRP is provided in [Appendix A.3](#).

Classical VRPs are special cases of FMDVRP: *TSP* is a VRP with a single vehicle and depot, *mTSP* is a VRP with multiple vehicles and a single depot, and *MDVRP* is a VRP with multiple vehicles and depots. Since FMVDRP is a general problem class, we learn a solver for FMVDRP and employ it to solve other specific problems (i.e., min-max MDVRP, min-max mTSP, and min-max CVRP), without retraining or fine-tuning. We demonstrate that the proposed method can solve these special cases almost optimally without retraining in [Section 4](#).

2.2 CROSS EXCHANGE

CE is a solution updating operator that iteratively improves the solution until it reaches a satisfactory result ([Taillard et al., 1997](#)). CE reduces the overall cost by *exchanging* the sub-tours in two tours. The CE operator is defined as:

$$\tau'_1, \tau'_2 = \text{CROSS}(a_1, b_1, a_2, b_2; \tau_1, \tau_2) \quad (2)$$

$$\tau'_1 \triangleq \tau_1[: a_1] \oplus \tau_2[a_2 : b_2] \oplus \tau_1[b_1 :] \quad (3)$$

$$\tau'_2 \triangleq \tau_2[: a_2] \oplus \tau_1[a_1 : b_1] \oplus \tau_2[b_2 :] \quad (4)$$

where τ_i and τ'_i are the input and updated tours of the vehicle i , respectively. $\tau_i[a : b]$ represents the sub-tour of τ_i , ranging from node a to b . $\tau \oplus \tau'$ represents the concatenation of tours τ and τ' . For brevity, we assume that node a_1, a_2 comes early than node b_1, b_2 in τ_1, τ_2 , respectively.

CE selects the sub-tours (i.e., $\tau_1[a_1 : b_1], \tau_2[a_2 : b_2]$) from τ_1, τ_2 and swaps the sub-tours to generate new tours τ'_1, τ'_2 . CE seeks to find the four points (a_1, b_1, a_2, b_2) to reduce the cost of the tours. For min-max VRPs, we define the cost of the two selected tours as $C(\tau_1, \tau_2) = \max(l(\tau_1), l(\tau_2))$, where $l(\tau_i)$ is the traveling distance of tour τ_i , and apply the CE operator to reduce this cost, i.e., $C(\tau'_1, \tau'_2) \leq C(\tau_1, \tau_2)$ in an attempt to minimize the traveling distance of the longest route. When the full search method is naively employed, the search cost is $\mathcal{O}(n^4)$, where n is the number of nodes in a tour.

[Fig. 1](#) illustrates how the improvement heuristics utilize CE to solve min-max FMDVRP. The improvement heuristics start by generating the initial feasible tours using simple heuristics. Then, they repeatedly (1) select two tours, (2) apply inter-operation to generate improved tours by CE, and (3) apply intra-operation to improve the tours independently. The improvement heuristics terminate when no more (local) improvement is possible.

Algorithm 2: NeuroCROSS operation

```

Input: tours  $\tau_1, \tau_2$ , cost-decrement prediction model  $f_\theta(\cdot)$ 
Output: updated tours  $\tau'_1, \tau'_2$ 
/* Predict cost decrement */
16  $\mathbb{S} \leftarrow \{\emptyset\}$ 
17 for  $(a_1, a_2) \in \tau_1 \times \tau_2$  do
18    $\hat{y}^*(a_1, a_2; \tau_1, \tau_2) \leftarrow f_\theta(a_1, a_2; \tau_1, \tau_2)$  // Cost-decrement prediction
19    $\mathbb{S} \leftarrow \mathbb{S} \cup \{(a_1, a_2), \hat{y}^*(a_1, a_2; \tau_1, \tau_2)\}$ 
/* Candidate set construction */
20 Sort  $\mathbb{S}$  by  $y^*(a_1, a_2; \tau_1, \tau_2)$  in the descending order
21  $\mathbb{S}_K \leftarrow$  Take first  $K$  elements of  $\mathbb{S}$ 
/* Perform search */
22  $a_1^* \leftarrow \emptyset, a_2^* \leftarrow \emptyset, b_1^* \leftarrow \emptyset, b_2^* \leftarrow \emptyset, y^* \leftarrow 0$ 
23 for  $((a_1, a_2), \hat{y}^*(a_1, a_2; \tau_1, \tau_2)) \in \mathbb{S}_K$  do
24    $(\bar{b}_1, \bar{b}_2) \leftarrow \arg \max_{b_1, b_2} (C(\text{CROSS}((a_1, b_1, a_2, b_2; \tau_1, \tau_2))) - C(\tau_1, \tau_2))$ 
25    $y^*(a_1, a_2; \tau_1, \tau_2) \leftarrow C(\text{CROSS}((a_1, \bar{b}_1, a_2, \bar{b}_2; \tau_1, \tau_2))) - C(\tau_1, \tau_2)$ 
26   if  $y^*(a_1, a_2; \tau_1, \tau_2) \geq y^*$  then
27      $a_1^* \leftarrow a_1, a_2^* \leftarrow a_2, b_1^* \leftarrow \bar{b}_1, b_2^* \leftarrow \bar{b}_2$ 
28      $y^* \leftarrow y^*(a_1, a_2; \tau_1, \tau_2)$ 
29  $(\tau'_1, \tau'_2) \leftarrow \text{CROSS}(a_1^*, b_1^*, a_2^*, b_2^*; \tau_1, \tau_2)$ 

```

3 NEURO CROSS EXCHANGE

In this section, we introduce Neuro CROSS exchange (NCE) to solve min-max FMDVRP and its special cases. The overall procedure of NCE is summarized in [Algorithm 1](#). We briefly explain `GetInitialSolution`, `SelectTours`, `NeuroCROSS`, and `IntraOperation`, and then provide the details of the proposed NeuroCROSS operation in the following subsections. NCE is particularly designed to improve the solution quality and problem solving speed of CE when solving min-max VRPs. Each component of NCE is as follows:

- **GetInitialSolution.** We use a multi-agent extended version of the greedy assignment heuristic ([Dell'Amico et al., 1993](#)) to obtain the initial feasible solutions. The heuristic first clusters the cities into $|\mathbb{V}|$ clusters and then applies the greedy assignment to each cluster to get the initial solution.
- **SelectTours.** Following the common practice, we select τ_1, τ_2 as the tours with the largest and smallest traveling distance (i.e., $\tau_1 = \arg \max_{\tau} (l(\tau_i)_{i \in \mathbb{V}})$, $\tau_2 = \arg \min_{\tau} (l(\tau_i)_{i \in \mathbb{V}})$).
- **NeuroCROSS.** We utilize the cost-decrement prediction model $f_\theta(\cdot)$ and two-stage search method to find the cost-improving tour pair (τ'_1, τ'_2) with $\mathcal{O}(n^2)$ budget. The details of the NCE operation will be given in [Sections 3.1](#) and [3.2](#).
- **IntraOperation.** For our target VRPs, the intra-operation is equivalent to solving TSP. We utilize `elkai` ([Dimitrovski](#)) to solve TSP.

3.1 NEURO CROSS EXCHANGE OPERATION

The CE operation can be shown as selecting two pairs of nodes (i.e., the pairs of a_1/b_1 and a_2/b_2) from the selected tours (i.e., τ_1, τ_2). This typically involves $\mathcal{O}(n^4)$ searches. To reduce the high search complexity, NCE utilizes the cost-decrement model $f_\theta(a_1, a_2; \tau_1, \tau_2)$ that predicts the maximum cost decrements from the given τ_1 and τ_2 , and the starting nodes a_1 and a_2 of their sub-tours. That is, $f_\theta(a_1, a_2; \tau_1, \tau_2)$ amortizes the search for the ending nodes b_1, b_2 given $(\tau_1, \tau_2, a_1, a_2)$, and helps to identify the promising (a_1, a_2) pairs that are likely to improve the tours. After selecting the top K promising pairs of (a_1, a_2) using $f_\theta(a_1, a_2; \tau_1, \tau_2)$, whose search cost is $\mathcal{O}(n^2)$, NCE then finds (b_1, b_2) to identify the promising (a_1, a_2) pairs. Overall, the entire search can be done in $\mathcal{O}(n^2)$. The following paragraphs detail the procedures of NCE.

Predicting cost decrement. We employ $f_\theta(a_1, a_2; \tau_1, \tau_2)$ (which will be explained in Section 3.2) to predict the optimal cost decrement y^* defined as:

$$y^*(a_1, a_2; \tau_1, \tau_2) = \max_{b_1, b_2} (C(\text{CROSS}((a_1, b_1, a_2, b_2; \tau_1, \tau_2))) - C(\tau_1, \tau_2)) \quad (5)$$

$$\approx f_\theta(a_1, a_2; \tau_1, \tau_2) \quad (6)$$

where $C(\tau_1, \tau_2) = \max(l(\tau_1), l(\tau_2))$. In other words, $f_\theta(\cdot)$ predicts the best cost decrement of τ_1 and τ_2 , given a_1 and a_2 . The real cost decrement labels are obtained from the real search operation.

Constructing search candidate set. By training $f_\theta(\cdot)$, we can amortize the search for b_1 and b_2 . However, this amortization bears the prediction errors, which can misguide entire improvement process. To alleviate this problem, we select the top K pairs of (a_1, a_2) that have the top K -largest y^* out of all (a_1, a_2) choices. Intuitively speaking, NCE exclude the less promising (a_1, a_2) pairs while utilizing the prediction model $f_\theta(\cdot)$ which can have some errors.

Performing reduced search. NCE finds the best (b_1, b_2) for each (a_1, a_2) in the search candidate sets and selects the best sub-tours (a_1, a_2, b_1, b_2) that maximizes the actual cost decrement (not prediction). Unlike the full search of CE, the proposed NCE only performs the search for (b_1, b_2) , which reduces the search cost from $\mathcal{O}(n^4)$ to $\mathcal{O}(n^2)$. The detailed procedures of NCE are summarized in [Algorithm 2](#).

3.2 COST-DECREMENT PREDICTION MODEL

NCE saves computations by employing $f_\theta(a_1, a_2; \tau_1, \tau_2)$ to predict $y^*(\cdot)$ from a_1, a_2, τ_1 and τ_2 . The overall procedure is illustrated in [Fig. 2](#).

Graph representation of (τ_1, τ_2) . We represent a pair of tours (τ_1, τ_2) as a directed complete graph $\mathcal{G} = (\mathbb{N}, \mathbb{E})$, where $\mathbb{N} = \tau_1 \cup \tau_2$ (i.e., the i^{th} node n_i of \mathcal{G} is either the city or depot of the tours, and e_{ij} is the edge from n_i to n_j). \mathcal{G} has the following node and edge features:

- $x_i = [\text{coord}(n_i), \mathbb{1}_{\text{depot}}(n_i)]$, where $\text{coord}(n_i)$ is the 2D Euclidean coordinate of n_i , and $\mathbb{1}_{\text{depot}}(n_i)$ is the indicator of whether n_i is a depot.
- $x_{ij} = [\text{dist}(n_i, n_j)]$, where $\text{dist}(n_i, n_j)$ is the 2D Euclidean distance between n_i and n_j .

Graph embedding with attentive graph neural network. We employ an attentive variant of graph-network (GN) block ([Battaglia et al., 2018](#)) to embed \mathcal{G} . The attentive embedding layer is defined as follows:

$$h'_{ij} = \phi_e(h_i, h_j, h_{ij}, x_{ij}) \quad (7)$$

$$z_{ij} = \phi_w(h_i, h_j, h_{ij}, x_{ij}) \quad (8)$$

$$w_{ij} = \text{softmax}(\{z_{ij}\}_{j \in \mathcal{N}(i)}) \quad (9)$$

$$h'_i = \phi_n(h_i, \sum_{j \in \mathcal{N}(i)} w_{ij} h'_{ij}) \quad (10)$$

where h_i and h_{ij} are node and edge embeddings respectively, ϕ_e , ϕ_w , and ϕ_n are the Multilayer Perceptron (MLP)-parameterized edge, attention and node operators respectively, and $\mathcal{N}(i)$ is the neighbor set of n_i . We utilize H embedding layers to compute the final node $\{h_i^{(H)} \mid n_i \in \mathbb{V}\}$ and edge $\{h_{ij}^{(H)} \mid e_{ij} \in \mathbb{E}\}$ embeddings.

Cost-decrement prediction. Based on the computed embedding, the cost prediction module ϕ_c predicts $y^*(a_1, a_2; \tau_1, \tau_2)$. The selection of the two starting nodes in τ_1 and τ_2 indicates (1) the addition of the two edges, $(a_1, a_2 + 1)$ and $(a_2, a_1 + 1)$, and (2) the removal of the original two edges, $(a_1, a_1 + 1)$ and $(a_2, a_2 + 1)$, as shown in the third block in [Fig. 2](#) (we overload the notations $a_1 + 1, a_2 + 1$ so that they denote the next nodes of a_1, a_2 in τ_1, τ_2 , respectively). To consider such edge addition and removal procedure in cost prediction, we design ϕ_c as follows:

$$\hat{y}^*(a_1, a_2; \tau_1, \tau_2) = \phi_c(\underbrace{h_{a_1}^{(H)}, h_{a_1+1}^{(H)}}_{\text{node embedding}}, \underbrace{h_{a_2}^{(H)}, h_{a_2+1}^{(H)}}_{\text{node embedding}}, \underbrace{h_{a_1, a_2+1}^{(H)}, h_{a_2, a_1+1}^{(H)}}_{\text{link addition}}, \underbrace{h_{a_1, a_1+1}^{(H)}, h_{a_2, a_2+1}^{(H)}}_{\text{link removal}}) \quad (11)$$

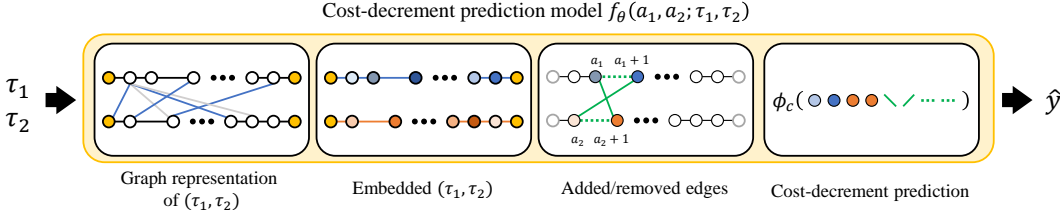


Figure 2: Cost-decrement prediction procedure

where $h_i^{(H)}$ and $h_{i,j}^{(H)}$ denotes the embedding of n_i and e_{ij} , respectively.

The quality of the NCE operator highly depends on the accuracy of f_θ . When $K \geq 10$, we experimentally confirmed that the NCE operator finds the argmax (a_1, a_2, b_1, b_2) pair with high probability. We provide the experimental details and results about the predictions of f_θ in [Appendix H](#).

4 EXPERIMENTS

This section provides the experiment results that validate the effectiveness of the proposed NCE in solving min-max FMDVRP and various min-max VRPs. To train $f_\theta(\cdot)$, we use the input $(\tau_1, \tau_2, a_1, a_2)$ and output y^* pairs obtained from 50,000 random min-max FMDVRP instances. The details of the train data generation are described in [Appendix G](#). The cost decrement model $f_\theta(\cdot)$ is parametrized by the GNN that contains the five attentive embedding layers. The details of the $f_\theta(\cdot)$ architecture and the computing infrastructure used to train $f_\theta(\cdot)$ are discussed in [Appendix G](#).

We emphasize that we use a single $f_\theta(\cdot)$ that is trained using data obtained from random min-max FMDVRP instances for all experiments. We found that $f_\theta(\cdot)$ effectively solves the three special cases (i.e., min-max MDVRP, min-max mTSP, and min-max CVRP) without retraining or fine-tuning, proving the effectiveness of NCE as a universal operator for VRPs.

4.1 MIN-MAX FMDVRP EXPERIMENTS

We evaluate the performance of NCE in solving various sizes of min-max FMDVRP. We consider 100 random min-max FMDVRP instances for each problem size (N_c, N_d, N_v) , where N_c, N_d, N_v are the number of cities, depots, and vehicles, respectively. We provide the average makespan and computation time for the 100 instances. For small-sized problems ($N_c \leq 10$), we employ CPLEX ([Cplex, 2009](#)) (an exact method), OR-tools ([Perron & Furnon](#)), CE (full search), ScheduleNet ([Park et al., 2021](#)), greedy heuristic ([Dell'Amico et al., 1993](#)), and greedy + TSP heuristic as baselines. For the larger-sized problems, we exclude CPLEX from the baselines due to its limited scalability. To our knowledge, our method is the first neural approach to solve min-max FMDVRP. Please note that we extend the ScheduleNet algorithm ([Park et al., 2021](#)), the most performing neural baseline for mTSP, and utilize it as a neural baseline for the min-max FMDVRP experiments.

Table 1: **FMDVRP results** (small-sized instances)

N_c, N_d (↓)	N_v (→) Method	2			3		
		Cost	Gap(%)	Time(sec.)	Cost	Gap(%)	Time(sec.)
(7,2)	CPLEX	1.543	0.00	0.31	1.363	0.00	0.83
	OR-tools	1.596	3.43	0.01	1.380	1.25	0.01
	CE	1.546	0.02	0.04	1.364	0.01	0.03
	NCE	1.546	0.02	0.10	1.365	0.01	0.12
(10,2)	N_v (→) Method	Cost	Gap(%)	Time(sec.)	Cost	Gap(%)	Time(sec.)
	CPLEX	1.745	0.00	9.29	1.488	0.00	63.00
	OR-tools	1.820	4.30	0.02	1.521	2.22	0.02
	CE	1.749	0.02	0.07	1.493	0.03	0.06
NCE	1.749	0.02	0.13	1.493	0.03	0.16	

Table 2: FMDVRP results (medium-sized instances)

N_c, N_d (↓)	$N_v(\rightarrow)$ Method	3			5			7		
		Cost	Gap(%)	Time(sec.)	Cost	Gap(%)	Time(sec.)	Cost	Gap(%)	Time(sec.)
(50,6)	OR-tools	2.39	15.46	2.20	1.56	10.64	2.44	1.27	6.72	2.58
	ScheduleNet	2.61	26.09	5.21	1.86	31.91	5.44	1.57	31.93	6.14
	Greedy	3.01	46.38	0.01	2.24	58.87	0.01	1.99	67.23	0.01
	Greedy + TSP	2.75	32.85	0.03	2.12	50.35	0.02	1.91	60.50	0.02
	CE	2.07	0.00	21.06	1.41	0.00	9.09	1.19	0.00	5.37
	NCE	2.08	0.48	1.26	1.40	-0.71	1.82	1.19	0.00	2.23
(100,8)	$N_v(\rightarrow)$ Method	5			7			10		
		Cost	Gap(%)	Time(sec.)	Cost	Gap(%)	Time(sec.)	Cost	Gap(%)	Time(sec.)
	OR-tools	2.00	14.94	30.46	1.51	12.69	32.25	1.20	10.09	34.38
	ScheduleNet	2.32	33.33	35.47	1.86	38.81	36.08	1.54	41.28	41.30
	Greedy	2.82	62.07	0.04	2.37	76.87	0.05	2.00	83.49	0.05
	Greedy + TSP	2.60	49.43	0.07	2.25	67.16	0.07	1.92	76.16	0.07
	CE	1.74	0.00	218.46	1.34	0.00	128.40	1.09	0.00	78.56
	NCE	1.75	0.57	6.41	1.34	0.00	9.54	1.09	0.00	13.34

Table 3: FMDVRP results (large-sized instances)

$N_c, N_d, N_v(\rightarrow)$ Method	200,10,10			400,20,20			600,30,30			800,40,40		
	Cost	Gap(%)	Time(sec.)	Cost	Gap(%)	Time(sec.)	Cost	Gap(%)	Time(sec.)	Cost	Gap(%)	Time(sec.)
OR-tools	1.47	12.21	418.8	1.08	12.50	9484	0.88	17.33	25967	1.09	67.69	72166
ScheduleNet	1.87	42.75	244.8	1.43	48.97	340	1.38	84.00	970	1.18	81.54	2383
Greedy	2.44	86.26	0.22	2.14	122.92	1.46	2.32	209.33	2.71	1.85	184.62	5.78
Greedy + TSP	2.28	74.05	0.32	2.06	114.58	1.54	2.20	193.33	2.90	1.75	169.23	6.05
NCE	1.31	0.00	70.96	0.96	0.00	520.5	0.75	0.00	1940	0.65	0.00	3802

Table 1 shows the performances of NCE on the small-sized problems. NCE achieve similar makespans with CPLEX (optimal solution) within significantly lower computation times. NCE outperforms OR-tools in terms of makespan but has longer computation time; however, the computation time for NCE will be much lower than that of OR-tools when the problem size becomes bigger. It is noteworthy that NCE exhibits larger computation time than CE as the forward-propagation cost of GNN is larger than exhaustive search for small problems.

Table 2 and Table 3 shows the performances of NCE on the medium and large-sized problems, respectively. Applying CPLEX for large min-max FMDVRPs is infeasible, so we exclude it from the baselines. Instead, the CE serves as an oracle to compute the makespans. For all cases, NCE provides a solution with almost zero gap from CE, but is computationally much faster. This validates that NCE successfully amortizes the search operations of CE with significantly lower computation times. In addition, NCE consistently outperforms OR-tools for both the makespan and computational time. The performance gap between NCE and OR-tools becomes more significant as N_c/N_v becomes large (i.e., each tour length becomes longer).

min-max MDVRP results. We also apply NCE with f_θ that is trained on FMDVRP to solve min-max MDVRP. As shown Tables A.1 to A.3 in Appendix B, NCE shows leading performance and is faster than the baselines, similar to the FMDVRP experiments.

4.2 MIN-MAX mTSP EXPERIMENTS

We evaluate the generalization capability of NCE for solving min-max mTSPs. We provide the average performance of 100 instances for each (N_c, N_v) pair. For the baselines, we consider two meta-heuristics; LKH-3 (Helsgaun, 2017), which is known as the one of the best mTSP heuristics, and OR-tools, and two neural baselines; ScheduleNet (Park et al., 2021) and DAN (Cao et al., 2021).

As shown in Table 4, NCE achieves similar performance with LKH-3 with significantly shorter computational time. It is noteworthy that LKH-3 employs mTSP-specific heuristics on top of LKH heuristics, while NCE does not employ any mTSP-specific structures. To validate the effect of task-specific information on NCE, we train NCE with mTSP data (NCE-mTSP) and solve mTSP. The performances of NCE and NCE-mTSP are almost identical, which indicates that NCE is highly generalizable. In addition, NCE consistently outperforms the neural baselines. We further apply

Table 4: **Average makespans of the random mTSPs:** DAN and ScheduleNet results are taken from the original papers, † computational time of DAN is measured with the Nvidia RTX 3090.

N_c (↓)	N_v (→) Method	5			7			10			
		Cost	Gap(%)	Time(sec.)	Cost	Gap(%)	Time(sec.)	Cost	Gap(%)	Time(sec.)	
50	LKH-3	2.00	0.00	187.46	1.95	0.00	249.31	1.91	0.00	170.20	
	OR-tools	2.04	2.00	3.24	1.96	0.51	3.75	1.91	0.00	3.67	
	DAN	2.29	14.50	0.25†	2.11	8.21	0.26†	2.03	6.28	0.30†	
	ScheduleNet	2.17	8.50	1.60	2.07	6.15	1.67	1.98	3.66	1.90	
	NCE	2.02	1.00	2.25	1.96	0.51	2.44	1.91	0.00	3.38	
	NCE-mTSP	2.02	1.00	2.48	1.96	0.51	2.50	1.91	0.00	3.44	
	<hr/>										
	100	LKH-3	2.20	0.00	262.85	1.97	0.00	474.78	1.98	0.00	378.90
OR-tools		2.41	9.55	35.47	2.03	3.05	45.40	2.03	2.53	48.86	
DAN		2.72	23.64	0.43†	2.17	10.15	0.48†	2.09	5.56	0.58†	
ScheduleNet		2.59	17.73	14.84	2.13	8.12	16.22	2.07	4.55	20.02	
NCE		2.25	2.27	16.01	1.98	0.51	12.22	1.98	0.00	24.08	
NCE-mTSP		2.24	1.82	16.36	1.97	0.00	13.00	1.98	0.00	23.37	
<hr/>											
200		LKH-3	2.04	0.00	1224.40	2.00	0.00	1147.13	1.97	0.00	908.14
	OR-tools	2.33	14.22	675.79	2.33	16.50	604.31	2.37	20.30	649.17	
	DAN	2.40	17.65	0.93†	2.20	10.00	0.98†	2.15	9.14	1.07†	
	ScheduleNet	2.45	20.10	193.41	2.24	12.00	213.07	2.17	10.15	225.50	
	NCE	2.06	0.98	83.82	2.00	0.00	72.32	1.97	0.00	113.74	
	NCE-mTSP	2.06	0.98	84.96	2.00	0.00	84.28	1.97	0.00	118.55	
	<hr/>										
	500	LKH-3	2.04	0.00	1224.40	2.00	0.00	1147.13	1.97	0.00	908.14
OR-tools		2.33	14.22	675.79	2.33	16.50	604.31	2.37	20.30	649.17	
DAN		2.40	17.65	0.93†	2.20	10.00	0.98†	2.15	9.14	1.07†	
ScheduleNet		2.45	20.10	193.41	2.24	12.00	213.07	2.17	10.15	225.50	
NCE		2.06	0.98	83.82	2.00	0.00	72.32	1.97	0.00	113.74	
NCE-mTSP		2.06	0.98	84.96	2.00	0.00	84.28	1.97	0.00	118.55	
<hr/>											
1000		LKH-3	2.04	0.00	1224.40	2.00	0.00	1147.13	1.97	0.00	908.14
	OR-tools	2.33	14.22	675.79	2.33	16.50	604.31	2.37	20.30	649.17	
	DAN	2.40	17.65	0.93†	2.20	10.00	0.98†	2.15	9.14	1.07†	
	ScheduleNet	2.45	20.10	193.41	2.24	12.00	213.07	2.17	10.15	225.50	
	NCE	2.06	0.98	83.82	2.00	0.00	72.32	1.97	0.00	113.74	
	NCE-mTSP	2.06	0.98	84.96	2.00	0.00	84.28	1.97	0.00	118.55	
	<hr/>										
	2000	LKH-3	2.04	0.00	1224.40	2.00	0.00	1147.13	1.97	0.00	908.14
OR-tools		2.33	14.22	675.79	2.33	16.50	604.31	2.37	20.30	649.17	
DAN		2.40	17.65	0.93†	2.20	10.00	0.98†	2.15	9.14	1.07†	
ScheduleNet		2.45	20.10	193.41	2.24	12.00	213.07	2.17	10.15	225.50	
NCE		2.06	0.98	83.82	2.00	0.00	72.32	1.97	0.00	113.74	
NCE-mTSP		2.06	0.98	84.96	2.00	0.00	84.28	1.97	0.00	118.55	
<hr/>											
5000		LKH-3	2.04	0.00	1224.40	2.00	0.00	1147.13	1.97	0.00	908.14
	OR-tools	2.33	14.22	675.79	2.33	16.50	604.31	2.37	20.30	649.17	
	DAN	2.40	17.65	0.93†	2.20	10.00	0.98†	2.15	9.14	1.07†	
	ScheduleNet	2.45	20.10	193.41	2.24	12.00	213.07	2.17	10.15	225.50	
	NCE	2.06	0.98	83.82	2.00	0.00	72.32	1.97	0.00	113.74	
	NCE-mTSP	2.06	0.98	84.96	2.00	0.00	84.28	1.97	0.00	118.55	
	<hr/>										
	10000	LKH-3	2.04	0.00	1224.40	2.00	0.00	1147.13	1.97	0.00	908.14
OR-tools		2.33	14.22	675.79	2.33	16.50	604.31	2.37	20.30	649.17	
DAN		2.40	17.65	0.93†	2.20	10.00	0.98†	2.15	9.14	1.07†	
ScheduleNet		2.45	20.10	193.41	2.24	12.00	213.07	2.17	10.15	225.50	
NCE		2.06	0.98	83.82	2.00	0.00	72.32	1.97	0.00	113.74	
NCE-mTSP		2.06	0.98	84.96	2.00	0.00	84.28	1.97	0.00	118.55	
<hr/>											
20000		LKH-3	2.04	0.00	1224.40	2.00	0.00	1147.13	1.97	0.00	908.14
	OR-tools	2.33	14.22	675.79	2.33	16.50	604.31	2.37	20.30	649.17	
	DAN	2.40	17.65	0.93†	2.20	10.00	0.98†	2.15	9.14	1.07†	
	ScheduleNet	2.45	20.10	193.41	2.24	12.00	213.07	2.17	10.15	225.50	
	NCE	2.06	0.98	83.82	2.00	0.00	72.32	1.97	0.00	113.74	
	NCE-mTSP	2.06	0.98	84.96	2.00	0.00	84.28	1.97	0.00	118.55	
	<hr/>										
	50000	LKH-3	2.04	0.00	1224.40	2.00	0.00	1147.13	1.97	0.00	908.14
OR-tools		2.33	14.22	675.79	2.33	16.50	604.31	2.37	20.30	649.17	
DAN		2.40	17.65	0.93†	2.20	10.00	0.98†	2.15	9.14	1.07†	
ScheduleNet		2.45	20.10	193.41	2.24	12.00	213.07	2.17	10.15	225.50	
NCE		2.06	0.98	83.82	2.00	0.00	72.32	1.97	0.00	113.74	
NCE-mTSP		2.06	0.98	84.96	2.00	0.00	84.28	1.97	0.00	118.55	
<hr/>											
100000		LKH-3	2.04	0.00	1224.40	2.00	0.00	1147.13	1.97	0.00	908.14
	OR-tools	2.33	14.22	675.79	2.33	16.50	604.31	2.37	20.30	649.17	
	DAN	2.40	17.65	0.93†	2.20	10.00	0.98†	2.15	9.14	1.07†	
	ScheduleNet	2.45	20.10	193.41	2.24	12.00	213.07	2.17	10.15	225.50	
	NCE	2.06	0.98	83.82	2.00	0.00	72.32	1.97	0.00	113.74	
	NCE-mTSP	2.06	0.98	84.96	2.00	0.00	84.28	1.97	0.00	118.55	
	<hr/>										
	200000	LKH-3	2.04	0.00	1224.40	2.00	0.00	1147.13	1.97	0.00	908.14
OR-tools		2.33	14.22	675.79	2.33	16.50	604.31	2.37	20.30	649.17	
DAN		2.40	17.65	0.93†	2.20	10.00	0.98†	2.15	9.14	1.07†	
ScheduleNet		2.45	20.10	193.41	2.24	12.00	213.07	2.17	10.15	225.50	
NCE		2.06	0.98	83.82	2.00	0.00	72.32	1.97	0.00	113.74	
NCE-mTSP		2.06	0.98	84.96	2.00	0.00	84.28	1.97	0.00	118.55	
<hr/>											
500000		LKH-3	2.04	0.00	1224.40	2.00	0.00	1147.13	1.97	0.00	908.14
	OR-tools	2.33	14.22	675.79	2.33	16.50	604.31	2.37	20.30	649.17	
	DAN	2.40	17.65	0.93†	2.20	10.00	0.98†	2.15	9.14	1.07†	
	ScheduleNet	2.45	20.10	193.41	2.24	12.00	213.07	2.17	10.15	225.50	
	NCE	2.06	0.98	83.82	2.00	0.00	72.32	1.97	0.00	113.74	
	NCE-mTSP	2.06	0.98	84.96	2.00	0.00	84.28	1.97	0.00	118.55	
	<hr/>										
	1000000	LKH-3	2.04	0.00	1224.40	2.00	0.00	1147.13	1.97	0.00	908.14
OR-tools		2.33	14.22	675.79	2.33	16.50	604.31	2.37	20.30	649.17	
DAN		2.40	17.65	0.93†	2.20	10.00	0.98†	2.15	9.14	1.07†	
ScheduleNet		2.45	20.10	193.41	2.24	12.00	213.07	2.17	10.15	225.50	
NCE		2.06	0.98	83.82	2.00	0.00	72.32	1.97	0.00	113.74	
NCE-mTSP		2.06	0.98	84.96	2.00	0.00	84.28	1.97	0.00	118.55	
<hr/>											
2000000		LKH-3	2.04	0.00	1224.40	2.00	0.00	1147.13	1.97	0.00	908.14
	OR-tools	2.33	14.22	675.79	2.33	16.50	604.31	2.37	20.30	649.17	
	DAN	2.40	17.65	0.93†	2.20	10.00	0.98†	2.15	9.14	1.07†	
	ScheduleNet	2.45	20.10	193.41	2.24	12.00	213.07	2.17	10.15	225.50	
	NCE	2.06	0.98	83.82	2.00	0.00	72.32	1.97	0.00	113.74	
	NCE-mTSP	2.06	0.98	84.96	2.00	0.00	84.28	1.97	0.00	118.55	
	<hr/>										
	5000000	LKH-3	2.04	0.00	1224.40	2.00	0.00	1147.13	1.97	0.00	908.14
OR-tools		2.33	14.22	675.79	2.33	16.50	604.31	2.37	20.30	649.17	
DAN		2.40	17.65	0.93†	2.20	10.00	0.98†	2.15	9.14	1.07†	
ScheduleNet		2.45	20.10	193.41	2.24	12.00	213.07	2.17	10.15	225.50	
NCE		2.06	0.98	83.82	2.00	0.00	72.32	1.97	0.00	113.74	
NCE-mTSP		2.06	0.98	84.96	2.00	0.00	84.28	1.97	0.00	118.55	
<hr/>											
10000000		LKH-3	2.04	0.00	1224.40	2.00	0.00	1147.13	1.97	0.00	908.14
	OR-tools	2.33	14.22	675.79	2.33	16.50	604.31	2.37	20.30	649.17	
	DAN	2.40	17.65	0.93†	2.20	10.00	0.98†	2.15	9.14	1.07†	
	ScheduleNet	2.45	20.10	193.41	2.24	12.00	213.07	2.17	10.15	225.50	
	NCE	2.06	0.98	83.82	2.00	0.00	72.32	1.97</			

sum of the traveling distance. The min-sum CVRP benchmark results are provided in [Appendix E, Table A.7](#).

4.4 ABLATION STUDIES

We evaluate the effects of the hyperparameters on NCE. The results are as follows:

- [Appendix F.1](#): the performance of NCE converges when the number of candidate $K \geq 10$.
- [Appendix F.2](#): the performance of NCE is less sensitive to the selection of intra solvers.
- [Appendix F.3](#): the performance of NCE is less sensitive to the selection of swapping tours.
- [Appendix F.4](#): the performance of NCE converges when the perturbation parameter $p \geq 5$.

5 RELATED WORKS

Supervised learning (SL) approach to solve VRPs SL approaches ([Joshi et al., 2019](#); [Vinyals et al., 2015](#); [Xin et al., 2021b](#); [Li et al., 2021](#); [2018](#)) utilize the supervision from the VRP solvers as the training labels. ([Vinyals et al., 2015](#); [Joshi et al., 2019](#)) imitates TSP solvers using PointerNet and graph convolution network (GCN), respectively. ([Joshi et al., 2019](#)) trains a GCN to predict the edge occurrence probabilities in TSP solutions. Even though SL often offer a faster solving speed than existing solvers, their use is limited to the problems where the solvers are available. Such property limits the use of SL from general and realistic VRPs.

Reinforcement learning (RL) approach to solve VRPs RL approaches ([Bello et al., 2016](#); [Khalil et al., 2017](#); [Nazari et al., 2018](#); [Kool et al., 2018](#); [Kwon et al., 2020](#); [Park et al., 2021](#); [Cao et al., 2021](#); [Guo et al., 2019](#); [Wu et al., 2019](#); [2021](#); [Falkner & Schmidt-Thieme, 2020](#); [Chen & Tian, 2019](#)) exhibit promising performances that are comparable to existing solvers as they learn solvers from the problem-solving simulations. ([Bello et al., 2016](#); [Nazari et al., 2018](#); [Kool et al., 2018](#); [Guo et al., 2019](#)) utilize an encoder-decoder structure to generate routing schedules sequentially, while ([Park et al., 2021](#); [Khalil et al., 2017](#)) use graph-based embedding to determine the next assignment action. However, RL approaches often require the problem-specific Markov decision process and network design. NCE does not require the simulation of the entire problem-solving. Instead, it only requires the computation of the swapping operation (i.e., the results of CE). This property allows NCE to be trained easily to solve various routing problems with one scheme.

Neural network-based (meta) heuristic approach Combining machine learning (ML) components with existing (meta) heuristics shows strong empirical performances when solving VRPs ([Hottung & Tierney, 2019](#); [Xin et al., 2021b](#); [Li et al., 2021](#); [Lu et al., 2019](#); [da Costa et al., 2021](#); [Kool et al., 2021](#)). They often employ ML to learn to solve NP-hard sub-problems of VRPs, which are difficult. For example, L2D ([Li et al., 2021](#)) learns to predict the objective value of CVRP, NLNS ([Hottung & Tierney, 2019](#)) learns a TSP solver when solving VRPs and DPDP ([Kool et al., 2021](#)) learns to boost the dynamic programming algorithms. To learn such solvers, these methods apply SL or RL. Instead, NCE learns the fundamental operator of meta-heuristics rather than predict or generate a solution. Hence, NCE that is trained on FMDVRP generalizes well to the special cases of FMDVRP. Furthermore, the training data for NCE can be prepared effortlessly.

6 CONCLUSION

We propose Neuro CROSS exchange (NCE), a neural network-enhanced CE operator, to learn a fundamental and universal operator that can be used to solve the various types of min-max VRPs. We validated that NCE can solve various min-max VRPs without retraining for each specific problem, exhibiting strong empirical performances. Although NCE addresses more realistic VRPs (i.e., min-max FMDVRP) than existing NCO solvers, NCE does not yet consider complex constraints such as pickup and delivery, and time windows. Our future research will focus on solving more complex VRPs by considering such various constraints during the NCE operation.

REFERENCES

- Peter W Battaglia, Jessica B Hamrick, Victor Bapst, Alvaro Sanchez-Gonzalez, Vinicius Zambaldi, Mateusz Malinowski, Andrea Tacchetti, David Raposo, Adam Santoro, Ryan Faulkner, et al. Relational inductive biases, deep learning, and graph networks. *arXiv preprint arXiv:1806.01261*, 2018.
- Irwan Bello, Hieu Pham, Quoc V Le, Mohammad Norouzi, and Samy Bengio. Neural combinatorial optimization with reinforcement learning. *arXiv preprint arXiv:1611.09940*, 2016.
- Jieyi Bi, Yining Ma, Jiahai Wang, Zhiguang Cao, Jinbiao Chen, Yuan Sun, and Yeow Meng Chee. Learning generalizable models for vehicle routing problems via knowledge distillation. *arXiv preprint arXiv:2210.07686*, 2022.
- Aigerim Bogrybayeva, Taehyun Yoon, Hanbum Ko, Sungbin Lim, Hyokun Yun, and Changhyun Kwon. A deep reinforcement learning approach for solving the traveling salesman problem with drone. *arXiv preprint arXiv:2112.12545*, 2021.
- Jakob Bossek, Pascal Kerschke, Aneta Neumann, Markus Wagner, Frank Neumann, and Heike Trautmann. Evolving diverse tsp instances by means of novel and creative mutation operators. In *Proceedings of the 15th ACM/SIGEVO Conference on Foundations of Genetic Algorithms*, pp. 58–71, 2019.
- Yuhong Cao, Zhanhong Sun, and Guillaume Sartoretti. Dan: Decentralized attention-based neural network to solve the minmax multiple traveling salesman problem. *arXiv preprint arXiv:2109.04205*, 2021.
- Xinyun Chen and Yuandong Tian. Learning to perform local rewriting for combinatorial optimization. In *Advances in Neural Information Processing Systems*, pp. 6281–6292, 2019.
- IBM ILOG Cplex. V12. 1: User’s manual for cplex. *International Business Machines Corporation*, 46(53):157, 2009.
- Paulo da Costa, Jason Rhuggenaath, Yingqian Zhang, Alp Akcay, and Uzay Kaymak. Learning 2-opt heuristics for routing problems via deep reinforcement learning. *SN Computer Science*, 2(5):1–16, 2021.
- Mauro Dell’Amico, Matteo Fischetti, and Paolo Toth. Heuristic algorithms for the multiple depot vehicle scheduling problem. *Management Science*, 39(1):115–125, 1993.
- Filip Dimitrovski. Elkai. URL <https://github.com/fikisipi/elkai>.
- Jonas K Falkner and Lars Schmidt-Thieme. Learning to solve vehicle routing problems with time windows through joint attention. *arXiv preprint arXiv:2006.09100*, 2020.
- Tiande Guo, Congying Han, Siqi Tang, and Man Ding. Solving combinatorial problems with machine learning methods. In *Nonlinear Combinatorial Optimization*, pp. 207–229. Springer, 2019.
- Keld Helsgaun. An extension of the lin-kernighan-helsgaun tsp solver for constrained traveling salesman and vehicle routing problems. *Roskilde: Roskilde University*, 2017.
- André Hottung and Kevin Tierney. Neural large neighborhood search for the capacitated vehicle routing problem. *arXiv preprint arXiv:1911.09539*, 2019.
- Yuan Jiang, Yaoxin Wu, Zhiguang Cao, and Jie Zhang. Learning to solve routing problems via distributionally robust optimization. *arXiv preprint arXiv:2202.07241*, 2022.
- Chaitanya K Joshi, Thomas Laurent, and Xavier Bresson. An efficient graph convolutional network technique for the travelling salesman problem. *arXiv preprint arXiv:1906.01227*, 2019.
- Elias Khalil, Hanjun Dai, Yuyu Zhang, Bistra Dilkina, and Le Song. Learning combinatorial optimization algorithms over graphs. In *Advances in Neural Information Processing Systems*, pp. 6348–6358, 2017.

- Minsu Kim, Jinkyoo Park, et al. Learning collaborative policies to solve np-hard routing problems. *Advances in Neural Information Processing Systems*, 34, 2021.
- Wouter Kool, Herke Van Hoof, and Max Welling. Attention, learn to solve routing problems! *arXiv preprint arXiv:1803.08475*, 2018.
- Wouter Kool, Herke van Hoof, Joaquim Gromicho, and Max Welling. Deep policy dynamic programming for vehicle routing problems. *arXiv preprint arXiv:2102.11756*, 2021.
- Yeong-Dae Kwon, Jinho Choo, Byoungjip Kim, Iljoo Yoon, Youngjune Gwon, and Seungjai Min. Pomo: Policy optimization with multiple optima for reinforcement learning. *Advances in Neural Information Processing Systems*, 33:21188–21198, 2020.
- Sirui Li, Zhongxia Yan, and Cathy Wu. Learning to delegate for large-scale vehicle routing. *Advances in Neural Information Processing Systems*, 34, 2021.
- Zhuwen Li, Qifeng Chen, and Vladlen Koltun. Combinatorial optimization with graph convolutional networks and guided tree search. *Advances in neural information processing systems*, 31, 2018.
- Ilya Loshchilov and Frank Hutter. Decoupled weight decay regularization. *arXiv preprint arXiv:1711.05101*, 2017.
- Hao Lu, Xingwen Zhang, and Shuang Yang. A learning-based iterative method for solving vehicle routing problems. In *International conference on learning representations*, 2019.
- Diganta Misra. Mish: A self regularized non-monotonic activation function. *arXiv preprint arXiv:1908.08681*, 2019.
- mTSPLib. mTSPLib. URL <https://profs.info.uaic.ro/~mtsplib/MinMaxMTSP/>.
- Mohammadreza Nazari, Afshin Oroojlooy, Lawrence Snyder, and Martin Takáč. Reinforcement learning for solving the vehicle routing problem. In *Advances in Neural Information Processing Systems*, pp. 9839–9849, 2018.
- Junyoung Park, Sanjar Bakhtiyar, and Jinkyoo Park. Schedulenet: Learn to solve multi-agent scheduling problems with reinforcement learning. *arXiv preprint arXiv:2106.03051*, 2021.
- Laurent Perron and Vincent Furnon. Or-tools. URL <https://developers.google.com/optimization/>.
- Quang Dung Pham, Kim Thu Le, Hoang Thanh Nguyen, Van Dinh Pham, and Quoc Trung Bui. A constraint-based local search for offline and online general vehicle routing. *International Journal on Artificial Intelligence Tools*, 26(02):1750004, 2017.
- Olçay Polat, Can B Kalayci, Osman Kulak, and Hans-Otto Günther. A perturbation based variable neighborhood search heuristic for solving the vehicle routing problem with simultaneous pickup and delivery with time limit. *European Journal of Operational Research*, 242(2):369–382, 2015.
- Éric Taillard, Philippe Badeau, Michel Gendreau, François Guertin, and Jean-Yves Potvin. A tabu search heuristic for the vehicle routing problem with soft time windows. *Transportation science*, 31(2):170–186, 1997.
- Son Van Nguyen, Dung Quang Pham, Trung Quoc Bui, and Hoang Thanh Nguyen. Solving min-max capacitated vehicle routing problem by local search. *Journal of Computer Science and Cybernetics*, 33(1):3–18, 2017.
- Oriol Vinyals, Meire Fortunato, and Navdeep Jaitly. Pointer networks. *Advances in neural information processing systems*, 28, 2015.
- Yaoxin Wu, Wen Song, Zhiguang Cao, Jie Zhang, and Andrew Lim. Learning improvement heuristics for solving the travelling salesman problem. 2019.
- Yaoxin Wu, Wen Song, Zhiguang Cao, Jie Zhang, and Andrew Lim. Learning improvement heuristics for solving routing problem. *IEEE Transactions on Neural Networks and Learning Systems*, 2021.

Liang Xin, Wen Song, Zhiguang Cao, and Jie Zhang. Multi-decoder attention model with embedding glimpse for solving vehicle routing problems. In *Proceedings of 35th AAAI Conference on Artificial Intelligence*, pp. 12042–12049, 2021a.

Liang Xin, Wen Song, Zhiguang Cao, and Jie Zhang. Neurokh: Combining deep learning model with lin-kernighan-helsgaun heuristic for solving the traveling salesman problem. *Advances in Neural Information Processing Systems*, 34, 2021b.

Neuro CROSS exchange

Supplementary Material

A MILP FORMULATIONS FOR MIN-MAX ROUTING PROBLEMS

This section provides the mixed integer linear programming (MILP) formulations of mTSP, MDVRP, and FMDVRP.

A.1 mTSP

mTSP is a multi-vehicle extension of the traveling salesman problem (TSP). mTSP comprises of a set of the nodes (i.e., cities) and depot V , a set of vehicles K , and a set of depot S . We define d_{ij} as the cost (or travel time) between node i and j , and the decision variable x_{ijk} denotes whether the edge between node i and j are taken by vehicle k . Following the convention, we consider mTSP with $|S| = 1$. The MILP formulation of mTSP is given as follows:

$$\text{minimize} \quad Q \tag{A.1}$$

$$\text{subject to.} \quad \sum_{i \in V} \sum_{j \in V} d_{ij} x_{ijk} \leq Q, \quad \forall k \in K : i \neq j, \tag{A.2}$$

$$\sum_{j \in V, i \neq j} x_{ijk} = 1, \quad \forall k \in K, \forall i \in S, \tag{A.3}$$

$$\sum_{i \in V, j \neq i} \sum_{k \in T} x_{ijk} = 1, \quad \forall j \in V \setminus S \tag{A.4}$$

$$\sum_{i \in V, i \neq j} x_{ijk} - \sum_{h \in V, h \neq j} x_{jhk} = 0, \quad \forall j \in V \setminus S \tag{A.5}$$

$$u_{ik} - u_{jk} + |V| x_{ijk} \leq |V| - 1, \quad \forall k \in K, j \in V \setminus S : i \neq j, \tag{A.6}$$

$$0 \leq u_{ik} \leq |V| - 1, \quad \forall k \in K, i \in V \setminus S \tag{A.7}$$

$$x_{ijk} \in \{0, 1\}, \quad \forall k \in K, \forall i, j \in V, \tag{A.8}$$

$$u_{ik} \in \mathbb{Z}, \quad \forall k \in K, i \in V \tag{A.9}$$

where Q denotes the longest traveling distance among multiple vehicles. (i.e., makespan), [Eq. \(A.3\)](#) indicates the vehicles start at the depot, [Eq. \(A.4\)](#) indicates that all cities are visited, [Eq. \(A.5\)](#) indicates the balance equation for all cities, [Eq. \(A.6\)](#) and [Eq. \(A.7\)](#) indicate the sub-tour eliminations.

A.2 MDVRP

Multi-depot VRP is a multi-depot extension of mTSP ([Appendix A.1](#)), where each vehicle starts from its own designated depot and returns to the depot. We extend the MILP formulation of mTSP to define the MILP formulation of MDVRP. On top of the mTSP formulation, we define K_i , which indicates the set of vehicles assigned to the depot i .

$$\text{minimize } Q \tag{A.10}$$

$$\text{subject to. } \sum_{i \in V} \sum_{j \in V} d_{ij} x_{ijk} \leq Q, \quad \forall k \in K : i \neq j, \tag{A.11}$$

$$\sum_{j \in V, j \neq i} \sum_{k \in T} x_{ijk} = 1, \quad \forall i \in V \setminus S \tag{A.12}$$

$$\sum_{i \in V, j \neq i} \sum_{k \in T} x_{ijk} = 1, \quad \forall j \in V \setminus S \tag{A.13}$$

$$\sum_{i \in V} x_{ijk} - \sum_{h \in V} x_{jhk} = 0, \quad \forall j \in V \setminus S, \forall k \in K \tag{A.14}$$

$$u_{ik} - u_{jk} + |V| x_{ijk} \leq |V| - 1, \quad \forall k \in K, j \in V \setminus S : i \neq j, \tag{A.15}$$

$$0 \leq u_{ik} \leq |V| - 1, \quad \forall k \in K, i \in V \setminus S \tag{A.16}$$

$$x_{ijk} \in \{0, 1\}, \quad \forall k \in K, \forall i, j \in V, \tag{A.17}$$

$$u_{ik} \in \mathbb{Z}, \quad \forall k \in K, i \in V \tag{A.18}$$

$$\sum_{j \in V \setminus S} x_{ijk} \leq 1, \quad \forall k \in K_i, \forall i \in S \tag{A.19}$$

$$\sum_{i \in V \setminus S} x_{ijk} \leq 1, \quad \forall k \in K_j, \forall j \in S \tag{A.20}$$

where [Eq. \(A.19\)](#) and [Eq. \(A.20\)](#) indicate that each vehicle starts and returns its own depot at most once.

A.3 FMDVRP

Flexible MDVRP (FMDVRP) is an extension of MDVRP, allowing the vehicle to return to any depot. We extend the MDVRP formulation (Appendix A.2) to define the FMDVRP formulation. To account for the flexibility of the returning depot, we introduce a dummy node for all depots; a depot is modeled with a start and return depot. We define S_1 and S_2 as the set of start and return depots and s_k as the start node of the vehicle k .

$$\text{minimize } Q \tag{A.21}$$

$$\text{subject to. } \sum_{i \in V} \sum_{j \in V} d_{ij} x_{ijk} \leq Q, \quad \forall k \in K : i \neq j, \tag{A.22}$$

$$\sum_{j \in V, j \neq i} \sum_{k \in T} x_{ijk} = 1, \quad \forall i \in V \setminus S \tag{A.23}$$

$$\sum_{i \in V, j \neq i} \sum_{k \in T} x_{ijk} = 1, \quad \forall j \in V \setminus S \tag{A.24}$$

$$\sum_{i \in V} x_{ijk} - \sum_{h \in V} x_{jhk} = 0, \quad \forall j \in V \setminus S, \forall k \in K \tag{A.25}$$

$$u_{ik} - u_{jk} + |V| x_{ijk} \leq |V| - 1, \quad \forall k \in K, j \in V \setminus S : i \neq j, \tag{A.26}$$

$$0 \leq u_{ik} \leq |V| - 1, \quad \forall k \in K, i \in V \setminus S \tag{A.27}$$

$$x_{ijk} \in \{0, 1\}, \quad \forall k \in K, \forall i, j \in V, \tag{A.28}$$

$$u_{ik} \in \mathbb{Z}, \quad \forall k \in K, i \in V \tag{A.29}$$

$$\sum_{j \in V \setminus S} x_{s_k j k} = 1, \quad \forall k \in K \tag{A.30}$$

$$\sum_{j \in V \setminus S} x_{ijk} = 0, \quad \forall k \in K, \forall i \in S \setminus s_k \tag{A.31}$$

$$\sum_{j \in V \setminus S} x_{ijk} \leq 1, \quad \forall k \in K, \forall i \in S_1 \tag{A.32}$$

$$\sum_{i \in V \setminus S} x_{ijk} \leq 1, \quad \forall k \in K, \forall j \in S_2 \tag{A.33}$$

$$\sum_{j \in V \setminus S} x_{ijk} = 0, \quad \forall k \in K, \forall i \in S_2 \tag{A.34}$$

$$\sum_{j \in V \setminus S} x_{ijk} = 0, \quad \forall k \in K, \forall i \in S_1 \tag{A.35}$$

$$\sum_{i \in S_1} \sum_{j \in V \setminus S} x_{ijk} = \sum_{i \in V \setminus S} \sum_{j \in S_2} x_{ijk}, \quad \forall k \in K \tag{A.36}$$

where Eqs. (A.30) and (A.31) indicate that each vehicle starts at its own depot. Eqs. (A.32) to (A.35) indicate the start and return depots constraints. Eq. (A.36) indicates the balance equation of the start and return depots.

B MIN-MAX MDVRP RESULTS

In this section, we provide the experiment results of MDVRP. We apply NCE with the f_θ trained on FMDVRP instances to solve MDVRP. For each (N_c, N_d, N_v) pair, we measure the average makespan of 100 instances. We provide the MDVRP results in Tables A.1 to A.3. Similar to the FMDVRP experiments, NCE shows leading performance while being faster than the baselines. From the results, we can conclude that the learned f_θ is transferable to the different problem sets. This phenomenon is rare in many ML-based approaches. It again highlights the effectiveness of learning fundamental operators (i.e., learn what should be cross exchanged) when solving the VRP families.

Table A.1: MDVRP results (small-sized instances)

N_c, N_d (↓)	$N_v(\rightarrow)$ Method	2			3		
		Cost	Gap(%)	Time(sec.)	Cost	Gap(%)	Time(sec.)
(7,2)	CPLEX	1.626	0.00	0.32	1.417	0.00	0.54
	OR-tools	1.704	4.80	0.01	1.433	1.13	0.01
	CE	1.626	0.00	0.05	1.418	0.01	0.04
	NCE	1.626	0.00	0.13	1.418	0.01	0.16
(10,2)	$N_v(\rightarrow)$ Method	Cost	Gap(%)	Time(sec.)	Cost	Gap(%)	Time(sec.)
	CPLEX	1.829	0.00	7.90	1.554	0.00	33.17
	OR-tools	1.926	5.30	0.02	1.590	2.32	0.02
	CE	1.829	0.00	0.09	1.558	0.03	0.08
	NCE	1.829	0.00	0.17	1.555	0.01	0.20

Table A.2: MDVRP results (medium-sized instances)

N_c, N_d (↓)	$N_v(\rightarrow)$ Method	3			5			7		
		Cost	Gap(%)	Time(sec.)	Cost	Gap(%)	Time(sec.)	Cost	Gap(%)	Time(sec.)
(50,6)	OR-tools	2.64	17.33	2.24	1.68	9.80	2.94	1.36	6.25	2.75
	CE	2.25	0.00	23.45	1.53	0.00	10.40	1.28	0.00	6.85
	NCE	2.25	0.00	2.08	1.53	0.00	2.63	1.28	0.00	2.93
	$N_v(\rightarrow)$ Method	Cost	Gap(%)	Time(sec.)	Cost	Gap(%)	Time(sec.)	Cost	Gap(%)	Time(sec.)
(100,8)	OR-tools	2.17	17.30	33.08	1.60	11.89	36.45	1.29	9.32	37.54
	CE	1.85	0.00	259.82	1.43	0.00	140.63	1.18	0.00	86.27
	NCE	1.86	0.54	11.61	1.43	0.00	11.96	1.18	0.00	15.70

Table A.3: MDVRP results (large-sized instances)

$N_c, N_d, N_v(\rightarrow)$ Method	200,10,10			400,20,20			600,30,30		
	Cost	Gap(%)	Time(sec.)	Cost	Gap(%)	Time(sec.)	Cost	Gap(%)	Time(sec.)
OR-tools	1.49	9.56	452.08	1.13	13.00	5179	1.01	24.69	22411
Greedy	2.99	119.85	0.20	2.77	177.00	0.93	3.20	295.06	2.69
Greedy + TSP	2.78	104.41	0.37	2.58	158.00	1.48	3.03	274.07	3.24
NCE	1.36	0.00	77.73	1.00	0.00	553.83	0.81	0.00	3173.5

C MIN-MAX MTSP RESULTS

In this section, we provide the additional experiment results of mTSP. We further apply NCE to solve mTSPLib (mTSPLib), which comprises of mTSP instances from real cities, and large scale problem. As reported in Table A.4 and Table A.5 NCE achieves the best results as compared to the baselines.

Table A.4: **mTSPLib results**: CPLEX results with * are optimal solutions. Otherwise, the known-best upper bound of CPLEX results are reported. The results of other baselines are taken from Park et al. (2021).

$N_c(\rightarrow)$	<i>Eil51</i>				<i>Berlin52</i>				<i>Eil76</i>				<i>Rat99</i>				Gap
	2	3	5	7	2	3	5	7	2	3	5	7	2	3	5	7	
CPLEX	222.7*	159.6	124.0	112.1	4110	3244	2441	2441	280.9*	197.3	150.3	139.6	728.8	587.2	469.3	443.9	1.00
LKH-3	222.7	159.6	124.0	112.1	4110	3244	2441	2441	280.9	197.3	150.3	139.6	728.8	587.2	469.3	443.9	1.00
OR-Tools	243.0	170.1	127.5	112.1	4665	3311	2482	2441	318.0	212.4	143.4	128.3	762.2	552.1	473.7	442.5	1.03
ScheduleNet	263.9	200.5	131.7	116.9	4826	3644	2758	2515	330.2	228.8	163.9	144.4	843.8	691.8	524.3	480.8	1.13
ScheduleNet (s.64)	239.3	173.5	125.8	112.2	4592	3276	2517	2441	317.7	220.8	153.8	131.7	781.2	627.1	502.3	464.4	1.05
DAN	274.2	178.9	158.6	118.1	5226	4278	2759	2697	361.1	251.5	170.9	148.5	930.8	674.1	504.0	466.4	1.18
DAN (s.64)	252.9	178.9	128.2	114.3	5098	3456	2677	2495	336.7	228.1	157.9	134.5	966.5	697.7	495.6	462.0	1.11
NCE	235.0	170.3	121.6	112.1	4110	3274	2660	2441	285.5	211.0	144.6	127.6	695.8	527.8	458.6	441.6	1.00
NCE-mTSP	226.1	166.3	119.9	112.1	4128	3191	2474	2441	282.1	197.5	147.2	127.6	666.0	533.2	462.2	443.9	0.98

Table A.5: **mTSP results** (large-sized instances)

$N_c(\rightarrow)$	Method	<i>mTSP300</i>			<i>mTSP500</i>			<i>mTSP750</i>		
		Cost	Gap(%)	Time(sec.)	Cost	Gap(%)	Time(sec.)	Cost	Gap(%)	Time(sec.)
LKH-3		2.12	0.00	1620	2.09	0.00	2981	1.99	0.00	6303
OR-tools		2.90	36.79	3605	7.63	265.07	9877	10.91	448.24	47225
ScheduleNet		2.25	6.13	689	2.17	3.83	3788	2.12	6.53	12199
Greedy		2.82	33.02	1.07	2.85	36.36	3.78	2.76	38.69	4.56
Greedy + TSP		2.80	32.08	1.39	2.84	35.89	4.48	2.75	38.19	5.53
NCE		2.12	0.00	301	2.09	0.00	583	1.99	0.00	580

D MIN-MAX CVRP RESULTS

We also provide min-max CVRP results for CVRPLib. We include two local search heuristic baselines N2 (Pham et al., 2017) and NMCF (Van Nguyen et al., 2017). We evaluate each instance 20 times and average it. As shown in Table A.6, NCE outperforms other Operation Research baselines in terms of computation speed and cost.

Table A.6: **CVRPLib result:** Results are taken from Van Nguyen et al. (2017)

Method VRP instance	<i>N2</i>			<i>NMCF</i>			<i>NCE (s.10)</i>		
	Cost	Gap(%)	Time(sec.)	Cost	Gap(%)	Time(sec.)	Cost	Gap(%)	Time(sec.)
E-n22-k4	110.00	-0.63	4.98	110.00	-0.63	3.62	110.70	0.00	2.51
E-n23-k3	242.10	0.04	20.50	243.45	0.60	27.35	242.00	0.00	14.09
E-n30-k3	192.95	0.63	53.72	192.45	0.37	10.85	191.75	0.00	10.45
E-n33-k4	244.15	0.00	85.87	244.00	-0.06	11.07	244.15	0.00	6.43
E-n51-k5	118.70	5.42	119.50	113.50	0.80	67.09	112.60	0.00	14.40
E-n76-k7	119.35	12.44	115.85	107.35	1.13	120.49	106.15	0.00	34.94
E-n76-k8	118.85	18.67	140.44	100.05	-0.10	94.57	100.15	0.00	31.27
E-n76-k10	117.40	23.71	149.21	99.55	4.90	31.69	94.90	0.00	34.94
E-n76-k14	111.10	27.12	146.64	93.60	7.09	27.22	87.40	0.00	42.13
E-n101-k8	141.65	26.42	140.07	117.05	4.46	69.01	112.05	0.00	71.96
E-n101-k14	113.25	13.19	161.05	101.50	1.45	68.04	100.05	0.00	83.74

E MIN-SUM CVRP RESULTS

In this section, we provide the results for min-sum CVRP benchmark instances. To solve min-sum CVRP, we trained NCE to predict min-sum cost decrement with $C(\tau_1, \tau_2)$ defined as $l(\tau_1) + l(\tau_2)$. As shown in Table A.7, NCE is on par with or outperforms other neural baselines. However, NCE is not efficient in terms of computation speed. This is because we initially design the CE operation to solve the min-max VRPs *not* min-sum VRPs. According to the experimental results, when CE operation is conducted to reduce the min-sum cost of two tours, it typically requires larger iterations to improve the solution to near optimum. This results indicates that other (local) search operator is required to efficiently solve the min-sum problems.

Table A.7: **CVRP benchmark results:** Best in **bold**; Second underline, (*s.n*) indicates the best results of *n* sampling, (*i.n*) indicates the best results after *n* improvement steps, and † indicates that the computation times of the neural baselines are measured with GPU. The run times of Lu et al. (2019) and Kwon et al. (2020) are taken from Kwon et al. (2020). The run times of the other neural baselines are taken from Kim et al. (2021).

Method	CVRP20			CVRP50			CVRP100		
	Cost	Gap(%)	Time(sec.)	Cost	Gap(%)	Time(sec.)	Cost	Gap(%)	Time(sec.)
LKH-3	6.14	0.00	0.72	10.38	0.00	2.52	15.65	0.00	4.68
OR-Tools	6.43	4.72	0.01	11.31	8.17	0.05	17.16	10.29	0.23
RL†(<i>s.10</i>) (Nazari et al., 2018)	6.40	4.23	0.16	11.15	7.46	0.23	16.96	8.39	0.45
AM†(<i>s.1280</i>) (Kool et al., 2018)	6.25	1.79	0.05	10.62	2.40	0.14	16.23	3.72	0.34
MDAM†(<i>s.50</i>) (Xin et al., 2021a)	6.14	0.00	0.03	10.48	0.96	0.09	15.99	2.17	0.32
POMO†(<i>s.8</i>) (Kwon et al., 2020)	6.14	0.00	0.01	10.42	0.35	0.01	<u>15.73</u>	0.43	0.01
NLNS†(<i>i.1280</i>) (Hottung & Tierney, 2019)	6.19	0.81	1.00	10.54	1.54	1.63	16.00	2.24	2.18
AM + LCP†(<i>s.1280</i>) (Kim et al., 2021)	6.16	0.33	0.09	10.54	1.54	0.20	16.03	2.43	0.45
Learn2OPT†(<i>i.2000</i>) (da Costa et al., 2021)	6.16	0.37	1.00	10.54	2.66	1.44	16.72	6.40	7.20
LIH†(<i>i.5000</i>) (Wu et al., 2021)	6.12	-0.33	0.72	10.45	0.67	1.44	16.03	2.43	1.80
NeuroRewriter† (Chen & Tian, 2019)	6.16	0.48	0.13	10.51	1.25	0.21	16.10	2.88	0.40
NCE	6.21	1.14	0.73	10.68	2.89	3.23	16.29	4.09	13.67
CE	6.21	1.14	0.77	10.69	2.99	11.11	16.28	4.03	79.12
NCE (<i>s.10, p.20</i>)	<u>6.13</u>	-0.16	3.99	<u>10.41</u>	0.29	20.17	15.81	1.02	90.12

F ABLATION STUDY

In this section, we provide the results of the ablation studies.

F.1 CANDIDATE SET

NCE constructed a search candidate set. To mitigate the prediction error of $f_{\theta}(\cdot)$ in finding the argmax of (a_1, a_2, b_1, b_2) , NCE search the top K pairs of (a_1, a_2) that have the largest y^* out of all (a_1, a_2) choices. We measure how the performance changes whenever the size of the candidate set K changes. As shown in Table A.8, as the size of K increases, the performance tends to increase slightly. When $K \geq 10$, the performance of NCE almost converges. Thus, we choose $K = 10$ as the default hyperparameter of NCE.

Table A.8: Effect of number of candidate

K	1		2		3		5		7		10		20		30	
	cost	time	cost	time	cost	time	cost	time	cost	time	cost	time	cost	time	cost	time
$(30,3,2)$	2.47	0.26	2.44	0.30	2.44	0.34	2.43	0.38	2.43	0.43	2.43	0.48	2.43	0.63	2.43	0.81
$(30,3,3)$	1.87	0.27	1.85	0.31	1.84	0.35	1.84	0.41	1.83	0.48	1.83	0.55	1.83	0.79	1.83	1.04
$(30,3,5)$	1.50	0.50	1.47	0.61	1.47	0.66	1.46	0.71	1.46	0.83	1.46	0.91	1.47	1.27	1.46	1.54
$(50,3,3)$	2.23	0.58	2.20	0.80	2.19	0.93	2.18	1.13	2.19	1.26	2.18	1.51	2.19	2.17	2.18	2.70
$(50,3,5)$	1.67	0.86	1.63	1.12	1.62	1.34	1.61	1.56	1.61	1.81	1.61	2.17	1.61	3.14	1.61	4.07
$(50,3,7)$	1.49	1.05	1.47	1.31	1.47	1.59	1.46	1.93	1.46	2.18	1.46	2.59	1.46	3.79	1.46	4.98

F.2 INTRA-SOLVER

NCE repeatedly applies the inter- and intra-operation. In this view, the choice of the intra-operation may affect the performance of NCE. In this subsection, we measured the performance of NCE according to intra-operation. We compare the results of NCE that uses Elkai, OR-tools, and 2-opt as the intra-operator. To solve TSP – the task intra-operator has to solve –, Elkai, OR-tools, and 2-opt show the best, second best, and third best performances. As shown in Table A.9, the performances of NCE are almost identical to the selection of an intra-operator. We validate that the effect of the intra-operation choice is negligible to the performance.

Table A.9: Effect of Intra TSP solver

N_c, N_d, N_v	$(30,3,2)$		$(30,3,3)$		$(30,3,5)$		$(50,3,3)$		$(50,3,5)$		$(50,3,7)$	
	cost	time	cost	time	cost	time	cost	time	cost	time	cost	time
2-opt	2.46	0.23	1.83	0.33	1.47	0.53	2.22	0.72	1.62	1.24	1.46	1.58
OR-tools	2.44	1.04	1.83	1.08	1.47	1.06	2.20	3.31	1.61	2.72	1.46	2.72
Elkai	2.43	0.41	1.83	0.55	1.46	0.69	2.18	1.55	1.61	2.17	1.46	2.13

F.3 SELECTING TWO VEHICLES

NCE chooses two tours for improvement during the iterative process. To understand the effect of the tour selection strategy, we measure the performance of NCE according to tour selection. We compare NCE results in a max-min selection case and a random selection case (i.e., pick two tours randomly). As shown in Table A.10, the performances of NCE are almost identical to the tour selection strategy. Therefore, we validate that the effect of the tour selection strategy is negligible.

Table A.10: Effect of selecting two vehicles

N_c, N_d, N_v	$(30,3,2)$		$(30,3,3)$		$(30,3,5)$		$(50,3,3)$		$(50,3,5)$		$(50,3,7)$	
	cost	time	cost	time	cost	time	cost	time	cost	time	cost	time
Random	2.43	0.42	1.84	0.61	1.48	0.94	2.18	1.43	1.62	2.39	1.47	2.62
Max-Min	2.43	0.41	1.83	0.55	1.46	0.69	2.18	1.55	1.61	2.17	1.46	2.13

F.4 PERTURBATION

NCE employs perturbation to increase performance. Perturbation is a commonly used strategy for enhancing the performance of meta-heuristics (Polat et al., 2015). It is done by randomly *perturbing* the solution and solving the problem with the perturbed solutions. This technique is beneficial to escape from the local optima. As described in Algorithm 1, when falling into the local optima, NCE randomly selects two tours and performs a random exchange. We compare the performance of NCE with different perturbations. As shown in Table A.11, the performance of NCE increases and converges as the number of perturbations p increases. When $p = 5$, the performance of NCE converges. Thus, we choose $p = 5$ as the default hyperparameter of NCE.

Table A.11: Effect of perturbation

P	0		1		2		3		5		7		10		20	
	cost	time	cost	time	cost	time	cost	time	cost	time	cost	time	cost	time	cost	time
$(30,3,2)$	2.50	0.12	2.48	0.17	2.46	0.22	2.44	0.27	2.43	0.38	2.43	0.49	2.42	0.69	2.41	1.34
$(30,3,3)$	1.89	0.16	1.86	0.22	1.84	0.30	1.84	0.35	1.83	0.55	1.82	0.61	1.81	0.81	1.81	1.42
$(30,3,5)$	1.49	0.29	1.48	0.33	1.48	0.43	1.47	0.50	1.47	0.67	1.46	0.85	1.46	1.25	1.46	2.28
$(50,3,3)$	2.26	0.31	2.24	0.49	2.22	0.65	2.19	0.81	2.18	1.28	2.17	1.83	2.16	2.61	2.14	4.83
$(50,3,5)$	1.66	0.52	1.64	0.77	1.63	0.94	1.62	1.24	1.61	1.97	1.61	2.59	1.60	3.61	1.59	6.53
$(50,3,7)$	1.48	0.85	1.48	1.04	1.47	1.43	1.47	2.02	1.46	2.65	1.46	2.95	1.46	3.77	1.45	6.44

G TRAINING DETAIL

Dataset preparation. To train the cost-decrement prediction model $f_\theta(\cdot)$, we generate 50,000 random FMDVRP instances. The random instance is generated by first sampling the number of customer N_c and depots N_d from $\mathcal{U}(10, 100)$ and $\mathcal{U}(2, 9)$ and $N_v = 2$ respectively, and then sampling the 2D coordinates of the cities from $\mathcal{U}(0, 1)$. As we set $N_v = 2$, we generate two tours by applying the initial solution construction heuristics explained in [Section 3.1](#). From τ_1, τ_2 , we compute the best true cost-decrements of all feasible (a_1, a_2) to prepare the training dataset. We generated 47,856,986 training samples from the 50,000 instances.

Hyperparameters. $f_\theta(\cdot)$ is parametrized via the GNN which employs five layers of the attentive embedding layer. We employ 4 layered MLPs to parameterize ϕ_e, ϕ_w, ϕ_n and ϕ_c , whose hidden dimensions and activation units are 64 and Mish ([Misra, 2019](#)). $f_\theta(\cdot)$ is trained to minimize the Huber loss for three epochs via AdamW ([Loshchilov & Hutter, 2017](#)) whose learning rate is fixed as 5×10^{-4} .

Computing resources. We run all experiments on the server equipped with AMD Threadripper 2990WX CPU and Nvidia RTX 3090 GPU. We use a single CPU core to evaluate all algorithms.

H EVALUATION OF THE COST DECREMENT MODEL

In this section, we evaluate the prediction accuracy of $f_\theta(\cdot)$. To evaluate $f_\theta(\cdot)$, we randomly generate 1,000 FMDVRP instances by sampling $N_C \sim \mathcal{U}(10, 100)$ and $N_D \sim \mathcal{U}(2, 9)$, and $(x, y) \sim \mathcal{U}(0, 1)^2$. From the instances, we measure the ratio of existence of the argmax (a_1, a_2) pair in the search candidate set whose size is K . As shown in Table A.12, when $K \geq 10$, NCE can find the argmax pair with at least 0.9 probability. We also provide the results of the cost-decrement predictions and its corresponding cost. As shown in Fig. A.1, $f_\theta(\cdot)$ predicts the general tendency well.

Table A.12: $f_\theta(\cdot)$ prediction performance test

K	1	3	5	10	20
argmax ratio (%)	42.9	71.3	78.6	90.9	97.4

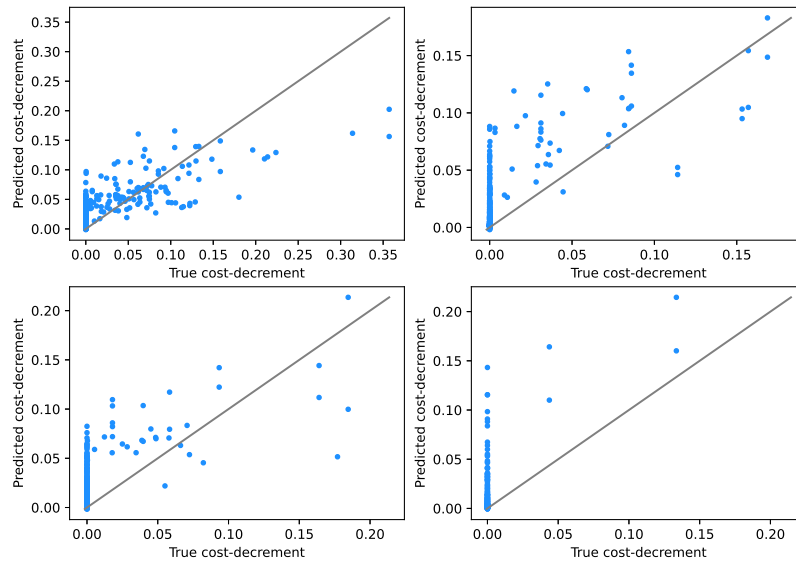


Figure A.1: Predicted cost-decrements vs. true cost-decrements

I COMPARISON WITH FULL SEARCH

To verify whether NCE successfully amortizes CE, we evaluate CE and NCE($K=10$, $p=0$) on FMDVRP. For the testing instances, we randomly generate 100 instances for each $N_c \in \{20, 30, 40, 50, 60, 70, 80, 90, 100\}$ with the fixed $N_d = 3$ and $N_v = 3$. As shown in Table A.13, NCE shows nearly identical performances with CE, but with significantly faster computation speed than CE as shown in Fig. A.2. We also test the mTSP and CVRP cases as shown in Table A.14.

Table A.13: **FMDVRP performance comparison of CE and NCE($K=10$, $p=0$)**

N_d, N_v	(3,3)									
	N_c	20	30	40	50	60	70	80	90	100
CE		1.651	1.893	2.088	2.257	2.384	2.531	2.695	2.811	2.929
NCE		1.651	1.891	2.088	2.262	2.390	2.530	2.697	2.806	2.934

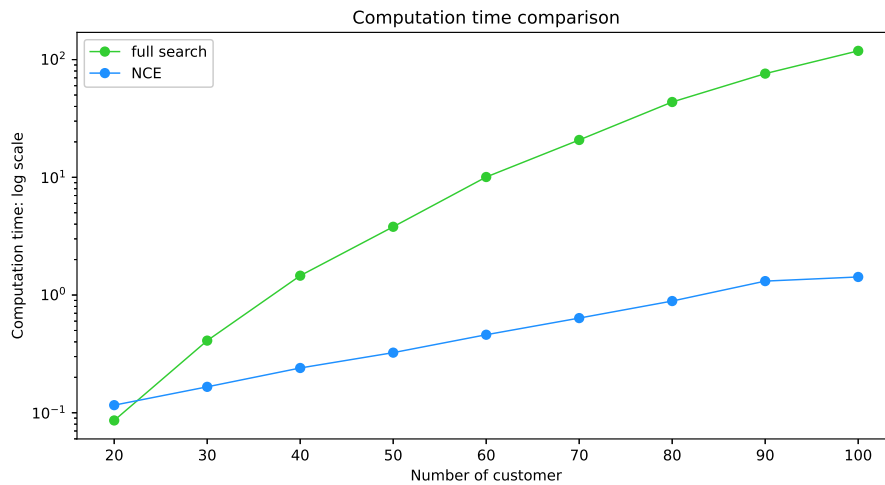


Figure A.2: Computation speed comparison

Table A.14: **mTSP, CVRP performance comparison of CE and NCE**

VRP instance	$mTSP50, N_v=5$		$mTSP100, N_v=10$		$mTSP200, N_v=15$		CVRP20		CVRP50		CVRP100	
	cost	time	cost	time	cost	time	cost	time	cost	time	cost	time
CE	2.02	11.35	1.97	87.28	2.00	414.9	6.21	0.96	10.91	11.38	16.23	80.23
NCE	2.02	2.48	1.97	13.00	2.00	84.28	6.21	0.57	10.90	2.93	16.23	14.08

J EXAMPLE SOLUTIONS

This section provides the routing examples. Fig. A.3 shows the solution of Rat99-2 computed by LKH-3 and NCE. Figs. A.4 and A.5 shows the solution of a FMDVRP and MDVRP instance computed by OR-Tools and NCE.

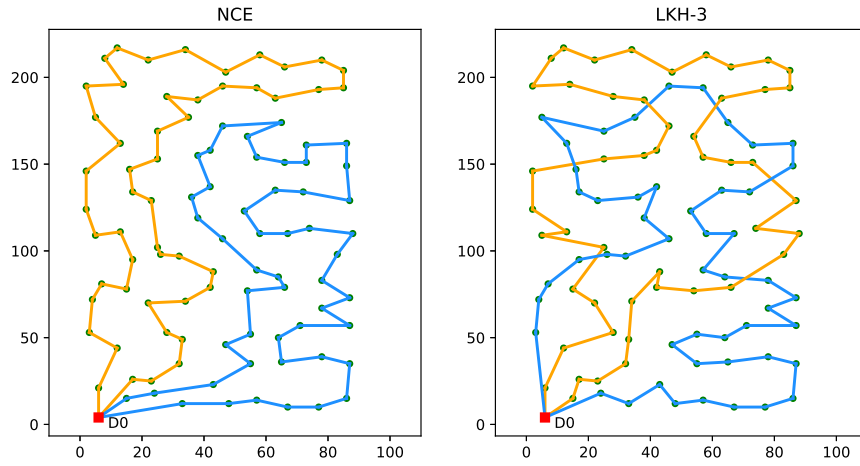


Figure A.3: Rat99-2 solutions computed by NCE and LKH-3

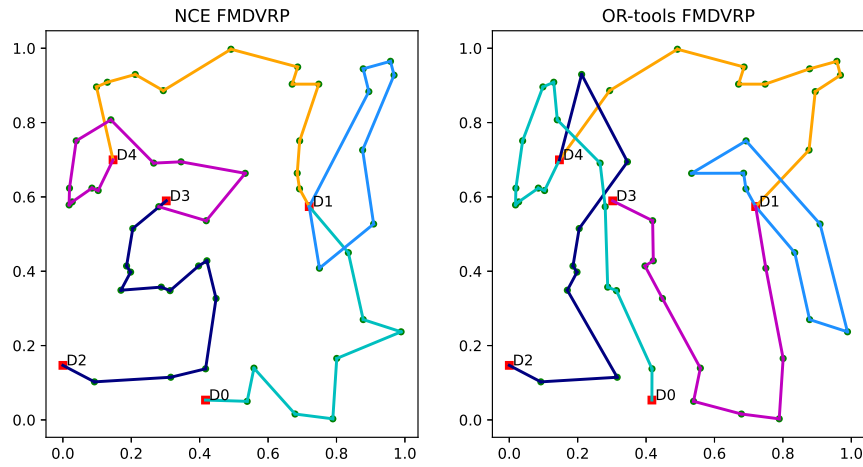


Figure A.4: FMDVRP solutions computed by NCE and OR-tools

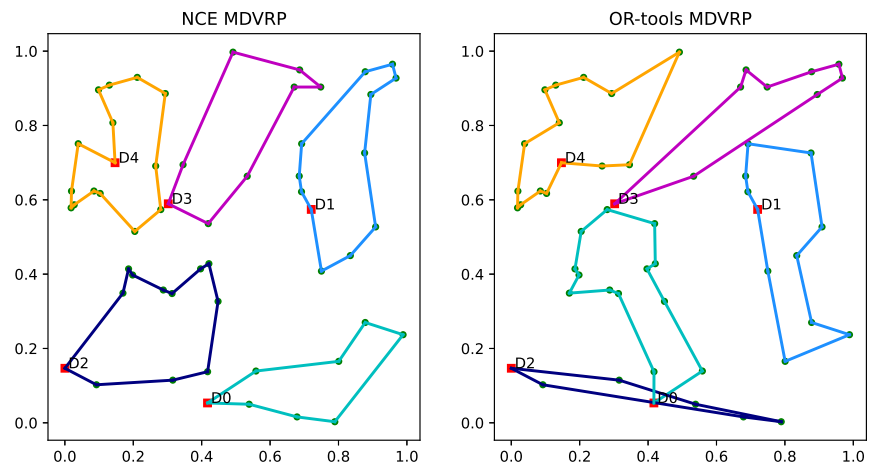


Figure A.5: MDVRP solutions computed by NCE and OR-tools

K CASE STUDY: PLANNING PATH FOR STERILIZING ROBOTS

We applied the trained NCE to solve a real-world application, the task of deriving the cooperative path for multiple sterilizing robots to sterilize the open space of a building in the minimum time. Here, the task nodes correspond to the spatial grids composing the entire building floor area, as shown in Fig. A.6. It consists of a total of 500 grids, of which 25 are obstacle areas (gray grids) that a robot cannot move into, and 99 are contaminated areas (orange grids) a robots need to sterilize. We assume the traveling time between the two adjacent grids is 1, the service time for the general area (green grids) is 1, and 2 for the contaminated areas. The upper left corner is the starting point. We formulate finding the cooperative paths for multiple robots to minimize the operation time as the min-max mTSP problem.

Fig. A.7 shows the path derived from NCE when there are 1 to 5 robots, and Table A.15 shows the time and objective value of solving the problem for each algorithm. The results show that the NCE algorithm trained using a synthetic dataset can produce an efficient cooperative path for multiple robots without retraining or fine-tuning. NCE reduces more than 10% of the makespan compared to Google OR-tool and 20% to Greedy+TSP when the number of robots is 5.

Note that the distribution of tasks is far from uniform distribution; each grid is clustered, and each cluster is separated due to the unique floor plan of a building. Thus, the experiment results verify the generalization capability of NCE to problem instances generated from a different distribution.

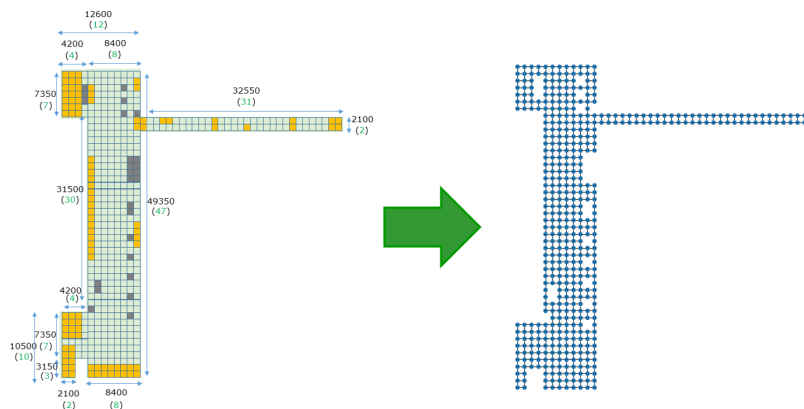


Figure A.6: Grid representation for the open space of the target building

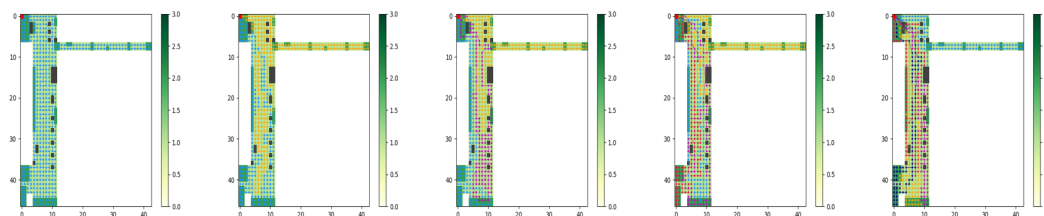


Figure A.7: NCE planned trajectories of the robots under different number of robots

Table A.15: Case study results

$N_r (\rightarrow)$ Method	1			2			3			4			5		
	Cost	Gap	Time	Cost	Gap	Time	Cost	Gap	Time	Cost	Gap	Time	Cost	Gap	Time
Greedy	1122	6.45	0.18	631	19.06	0.21	458	25.48	0.24	362	24.83	0.28	306	24.90	0.29
Greedy + TSP	1054	0.00	30.61	591	11.51	14.33	432	18.36	9.75	349	20.34	5.83	294	20.00	4.51
OR-tools	1066	1.14	553.2	573	8.11	1624.6	383	4.93	1554.7	306	5.52	2052.5	269	9.80	1043.8
NCE	1054	0.00	30.6	530	0.00	450.7	365	0.00	361.7	290	0.00	383.8	245	0.00	233.2

L BALANCE BETWEEN PERFORMANCE AND COMPUTATION TIME

Because NCE is an improvement heuristic, the more computation time is used, the better outcome will be produced. Thus, we investigate how the performance varies with the allowed computation time. We sampled 100 instances of FMDVRP $(N_c, N_d, N_v)=(60, 5, 5)$ and computed the average cost and computation time of NCE and baselines on these problem instances.

Fig. A.8 depicts the relationships between “Run time (computational cost) vs. Cost curve” in the form of a Pareto curve for the case of FMDVRP $(N_c, N_d, N_v)=(60, 5, 5)$. The result shows how the performance of NCE improves with more computation time, and this trend is always superior to another baseline.

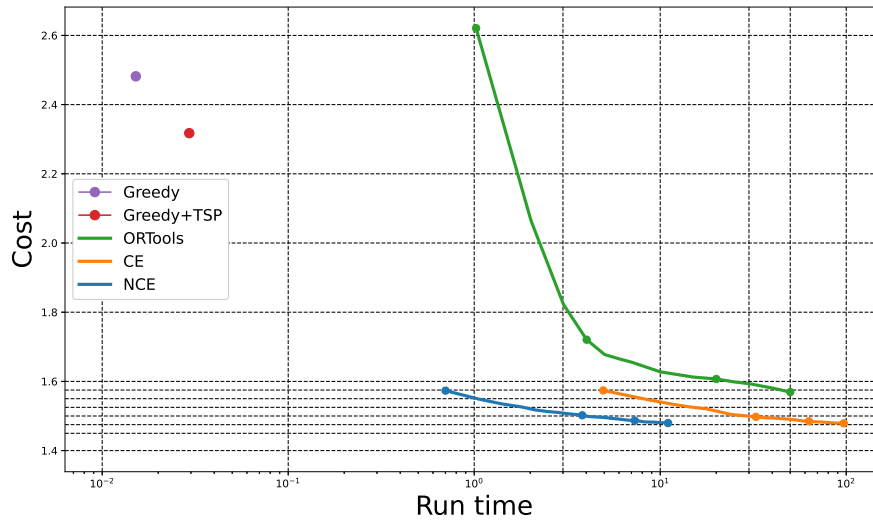


Figure A.8: Performance vs Computation time curve

M GENERALIZATION TO DIFFERENT DISTRIBUTION

We investigate the generalization capability of NCE to the problem instances generated from different distributions. We have employed the NCE trained by FMDVRP random instances to the problems generated by the different distributions introduced in (Bi et al., 2022). We used cluster, expansion, explosion, grid, implosion, and mixed distribution as unseen distributions for testing. We followed the definition in the (Bossek et al., 2019; Jiang et al., 2022; Bi et al., 2022), and the data were taken from the (Bi et al., 2022).

Table A.16 summarizes the experiment result. As in the case of uniform distribution, NCE shows leading performance while being faster than OR-Tools and CE. Note that we did not retrain our NCE algorithm but just employed the already trained existing NCE algorithm to new distribution tasks. From the results, we can conclude that the learned f_θ is generalizable to the different distributions other than the uniform. It again highlights the effectiveness of learning fundamental operators when solving the VRP families.

Table A.16: Results from various distributions

$N_c, N_d, N_v(\rightarrow)$		FMDVRP (46,5,5)								
Distribution Method	Cluster			Expansion			Explosion			
	Cost	Gap(%)	Time(sec.)	Cost	Gap(%)	Time(sec.)	Cost	Gap(%)	Time(sec.)	
OR-tools	0.92	4.55	1.92	1.25	6.90	1.75	1.33	9.92	1.75	
Greedy	1.32	50.00	0.01	1.94	67.24	0.01	1.96	61.98	0.01	
Greedy + TSP	1.25	42.05	0.02	1.82	56.90	0.02	1.86	53.72	0.02	
CE	0.88	0.00	5.82	1.16	0.00	6.50	1.39	0.00	6.39	
NCE	0.88	0.00	1.51	1.16	0.00	1.39	1.21	0.00	1.64	
Distribution Method	Grid			Implosion			Mixed			
	Cost	Gap(%)	Time(sec.)	Cost	Gap(%)	Time(sec.)	Cost	Gap(%)	Time(sec.)	
OR-tools	1.51	7.86	1.79	1.52	9.35	1.79	1.36	7.09	1.91	
Greedy	2.27	62.14	0.01	2.20	58.27	0.01	2.06	62.20	0.01	
Greedy + TSP	2.16	54.29	0.02	2.10	51.08	0.02	1.95	53.54	0.02	
CE	1.41	0.71	6.07	1.39	0.00	6.34	3.03	0.00	7.41	
NCE	1.40	0.00	1.77	1.39	0.00	1.84	1.27	0.00	1.90	
$N_c, N_d, N_v(\rightarrow)$		FMDVRP (94,7,7)								
Distribution Method	Cluster			Expansion			Explosion			
	Cost	Gap(%)	Time(sec.)	Cost	Gap(%)	Time(sec.)	Cost	Gap(%)	Time(sec.)	
OR-tools	0.91	5.81	24.86	1.16	7.41	23.37	1.21	10.00	24.25	
Greedy	1.41	63.95	0.04	1.92	77.78	0.04	1.97	79.09	0.04	
Greedy + TSP	1.35	56.98	0.08	1.81	67.59	0.07	1.84	67.27	0.06	
CE	0.86	0.00	105.66	1.08	0.00	104.06	1.10	0.00	105.82	
NCE	0.86	0.00	9.11	1.08	0.00	8.60	1.10	0.00	9.70	
Distribution Method	Grid			Implosion			Mixed			
	Cost	Gap(%)	Time(sec.)	Cost	Gap(%)	Time(sec.)	Cost	Gap(%)	Time(sec.)	
OR-tools	1.50	9.49	25.14	1.49	11.19	24.13	1.37	7.87	27.94	
Greedy	2.38	73.72	0.04	2.35	75.37	0.04	2.26	77.95	0.04	
Greedy + TSP	2.24	63.50	0.06	2.23	66.42	0.06	2.15	69.29	0.07	
CE	1.37	0.00	98.27	1.34	0.00	98.55	1.27	0.00	148.73	
NCE	1.37	0.00	9.24	1.34	0.00	9.49	1.27	0.00	10.11	